



Universiteit  
Leiden  
The Netherlands

## **Irradiation induced biochemical changes in human mandibular bone: a Raman Spectroscopic study**

Padala, S.R.; Saikia, D.; Mikkonen, J.J.W.; Uurasjarvi, E.; Dekker, H.; Schulten, E.A.J.M.; ... ; Kullaa, A.M.

### **Citation**

Padala, S. R., Saikia, D., Mikkonen, J. J. W., Uurasjarvi, E., Dekker, H., Schulten, E. A. J. M., ... Kullaa, A. M. (2022). Irradiation induced biochemical changes in human mandibular bone: a Raman Spectroscopic study. *Applied Spectroscopy*, 76(10), 1165-1173.  
doi:10.1177/00037028221109244

Version: Publisher's Version

License: [Licensed under Article 25fa Copyright Act/Law \(Amendment Taverne\)](#)

Downloaded from: <https://hdl.handle.net/1887/3563497>

**Note:** To cite this publication please use the final published version (if applicable).

# Irradiation Induced Biochemical Changes in Human Mandibular Bone: A Raman Spectroscopic Study

Applied Spectroscopy  
2022, Vol. 76(10) 1165–1173  
© The Author(s) 2022  
Article reuse guidelines:  
[sagepub.com/journals-permissions](https://sagepub.com/journals-permissions)  
DOI: 10.1177/00037028221109244  
[journals.sagepub.com/home/asp](https://journals.sagepub.com/home/asp)  
SAGE

Sridhar Reddy Padala<sup>1,†</sup>, Dimple Saikia<sup>2,†</sup>, Jopi J. W. Mikkonen<sup>1,3</sup>, Emilia Uurasjärvi<sup>3</sup>, Hannah Dekker<sup>4</sup>, Engelbert A. J. M. Schulten<sup>4</sup> , Nathalie Bravenboer<sup>5,6</sup>, Arto Koistinen<sup>3</sup>, Amrita Chauhan<sup>2</sup>, Surya P. Singh<sup>2</sup>  and Arja M. Kullaa<sup>1</sup> 

## Abstract

Understanding the biochemical changes in irradiated human mandible after radiotherapy of cancer patients is critical for oral rehabilitation. The underlying mechanism for radiation-associated changes in the bone at the molecular level could lead to implant failure and osteoradionecrosis. The study aimed to assess the chemical composition and bone quality in irradiated human mandibular bone using Raman spectroscopy. A total of 33 bone biopsies from 16 control and 17 irradiated patients were included to quantify different biochemical parameters from the Raman spectra. The differences in bone mineral and matrix band intensities between control and irradiated groups were analyzed using unpaired Student's *t*-test with statistical significance at  $p < 0.05$ . Findings suggest that the intensity of the phosphate band is significantly decreased and the carbonate band is significantly increased in the irradiated group. Further, the mineral crystallinity and carbonate to phosphate ratio are increased. The mineral to matrix ratio is decreased in the irradiated group. Principal component analysis (PCA) based on the local radiation dose and biopsy time interval of irradiated samples did not show any specific classification between irradiation sub-groups. Irradiation disrupted the interaction and bonding between the organic matrix and hydroxyapatite minerals affecting the bone biochemical properties. However, the normal clinical appearance of irradiated bone would have been accompanied by underlying biochemical and microscopical changes which might result in radiation-induced delayed complications.

## Keywords

Biochemical, irradiation, mandible, osteoradionecrosis, Raman spectroscopy

Date received: 17 February 2022; accepted: 25 May 2022

## Introduction

Radiotherapy (RT) is considered one of the treatment regimes for the clinical management of head and neck malignancies after surgery. RT involves exposure of the affected site with high-energy ionizing radiation to control or kill the cancer cells. It has contributed effectively to improving the treatment rates in many types of cancer.<sup>1</sup> Though RT plays an important role in the treatment of head and neck malignancies, its associated effects with acute and late complications can have an impact on the outcome of oral rehabilitation. Radiation administration results in negative sequelae (xerostomia, mucositis, etc.) in soft tissue and substantial damage to the bone including pathologic fracture and osteoradionecrosis.<sup>2</sup> Placing dental implants in essential irradiated tissue is a clinical challenge: Peri-implantitis and osteoradionecrosis (ORN) are frequently observed, resulting in implant loss in up to 23% of patients.<sup>3,4</sup> The severity of the bone alteration ranges from

<sup>1</sup>Institute of Dentistry, University of Eastern Finland, Kuopio, Finland

<sup>2</sup>Department of Bio-Sciences and Bio-Engineering, Indian Institute of Technology, Dharwad, India

<sup>3</sup>SIB Labs, University of Eastern Finland, Kuopio, Finland

<sup>4</sup>Department of Oral and Maxillofacial Surgery/Oral Pathology, Amsterdam UMC and Academic Centre for Dentistry Amsterdam (ACTA), Vrije Universiteit Amsterdam, De Boelelaan, The Netherlands

<sup>5</sup>Department of Clinical Chemistry, Amsterdam UMC, Vrije Universiteit Amsterdam, De Boelelaan, The Netherlands

<sup>6</sup>Department of Internal Medicine, Division of Endocrinology and Center for Bone Quality, Leiden University Medical Center, Leiden, The Netherlands

<sup>†</sup>Authors contributing equally

### Corresponding author:

Arja M. Kullaa, Institute of Dentistry, University of Eastern Finland, Yliopistonranta 1, Kuopio 70211, Finland.

Email: [arja.kullaa@uef.fi](mailto:arja.kullaa@uef.fi)

temporary bone loss, reduced growth, and poor healing to fragility fractures that may not occur until several months or years after the primary RT treatment.<sup>5,6</sup> Irradiation can disturb the bone cells and can directly injure the bone progenitor cells which affects the nature of the bone matrix since bone resorption and remodeling depends on these cells.<sup>7</sup> The loss of trabecular bone and resultant changes in the structural properties of the remaining bone fail to explain the biomechanical weakening of the bone indicating some intrinsic material abnormality in the irradiated bone.<sup>8</sup> In our recent study, a description of the cellular and vascular response to RT has been drawn from canine irradiation models, showing compatible osseointegrated implants.<sup>9</sup>

Various invasive and noninvasive techniques have been introduced to assess the radiation-induced effects. Among all, optical spectroscopy methods based on fluorescence, infrared, and Raman spectroscopy have the potential to serve as an alternate approach for bone analysis.<sup>10</sup> Raman spectroscopy is a nondestructive, rapid analysis technique that requires only small sample volumes and is resistant to interference from water.<sup>11</sup> It is a powerful tool for measuring bone compositional information in form of mineral to matrix ratio (MMR), mineral crystallinity, carbonate content, collagen cross-linking ratio, and depolarization ratios of mineral and collagen fibril, which are unavailable using established histological and imaging techniques. Alterations in these parameters could help to elucidate the radiation-induced changes in bone material behavior and evaluate the efficacy of radioprotective therapies.<sup>12</sup>

Raman shifts or bands corresponding to specific components of the bone can provide valuable insight into the pathophysiological events in an irradiated bone.<sup>13</sup> Previous biochemical analytic studies indicated that irradiated bone is characterized by altered material properties and abnormalities in the chemical composition and structure of the bone matrix.<sup>14–16</sup> In irradiated hindlimb mouse models, bone mineral and matrix compositions were studied using Raman spectroscopy. These animal studies demonstrated changes in the bone quality and its mechanical competence contributing toward fragility fractures.<sup>17–19</sup> A Raman study by Barth et al.<sup>20</sup> revealed a large increase in the amide I peak height after irradiation implying damage to the collagen associated with increased crosslinking. The chemical composition and ultrastructure of the irradiated mandible and tibia showed differences in the physiology and biochemical properties.<sup>8,13</sup>

For oral rehabilitation after RT in head and neck cancer patients, understanding intrinsic biochemical changes including both chemical composition and degree of molecular orientation in the irradiated bone is essential. Due to multifactorial radiation-induced changes in the bone, and limited literature, there is still a need to study irradiated human jawbone. This study aims to investigate the biochemical and compositional alterations in human mandibular bone after irradiation using Raman spectroscopy. We also intend to increase the current understanding by assessing the dose-related biochemical changes in irradiated bone.

## Materials and Methods

### Subjects

A total of 33 bone biopsy samples were harvested during the dental implant surgery from the mandible of the control (C) and irradiated group (IR) patients. The irradiated group consisted of 17 patients (13 males, four females; range 51–79 years, the mean age of 64.1 years), with a history of RT for head and neck malignancy, and underwent oral rehabilitation with dental implants in the mandible. The control group consisted of 16 fully edentulous and clinically healthy patients, without a history of cancer and RT. Of these 16 patients, six were males and 10 were females with the age range of 33–74 years (mean age 60.9 years). The female subjects selected in this study were of post-menopausal age (over 50 years), to improve the sample homogeneity. Exclusion criteria included impaired bone metabolism (e.g., hyperparathyroidism, osteomalacia), bisphosphonate medication, or systemic immunosuppressive medication up to three months before sample harvesting. All patients had normal blood calcium, phosphate, parathyroid hormone, and HbA1c levels.

To evaluate the differential radiation dose-induced effects in the mandible, the irradiated patients were subdivided based on local dose into Groups 1 and 2. Group 1 was consisting of subjects exposed to radiation dose <50 Gy and Group 2 with patients ≥50 Gy. All patients who had received an estimated dose of 50 Gy or higher on the anterior mandible were treated with 20 sessions of hyperbaric oxygen therapy preoperatively and 10 sessions postoperatively (Marx protocol) as a standard procedure. Also, we divided the irradiated patients based on the radiation-biopsy time interval into Group A: <60 months and Group B: >60 months to assess the early and delayed mandibular bone changes. The demographic data, radiation dose details, and timing from the radiation to biopsy are mentioned in [Table I](#).

Before the study, the Medical Ethical Committee of the Amsterdam University Medical Centers (location VU Medical Center, Amsterdam, the Netherland (Registration number 2011/220) and the Research Ethics Committee of the Northern Savo Hospital District (754/2018) provided approval for the present research. Written informed consent was obtained from all individual participants included in the study.

### Bone Sample Harvesting and Specimen Preparation

The patients in the control group were given a single dose of antibiotic prophylaxis (amoxicillin, 3 gm orally) before the dental surgical procedure. The surgery was performed under local anesthesia by a single oral and maxillofacial surgeon in the Alrijne Hospital in Leiderdorp, The Netherlands. The irradiated group was treated in the Department of Oral and Maxillofacial Surgery, Amsterdam University Medical Centers (Amsterdam UMC), location Vrije Universiteit Medical Center (VUmc), in Amsterdam, The Netherlands. The

**Table I.** Demographic data of study groups.

	Patients n = 33	Male/ female	Age range (mean)	Total dose (mean)	Local dose <sup>a</sup> (mean)		Radiation biopsy interval (mean)	
Irradiated group	17	13M/4F	51–79 yrs (64.1)	54–70 Gy (66.5)	15–70 Gy (43.9) Group 1 <50 Gy 6 patients		11–199 months (63.1) Group A < 60 months 10 patients	
Control group	16	6M/10F	33–74 yrs (60.9)	—	Group 2 ≥50 Gy 6 patients		Group B > 60 months 7 patients	

<sup>a</sup>Data is not available for five cases because the radiation biopsy interval was more than 10 years

operation was done under general anesthesia and patients were given antibiotic prophylaxis following ORN protocol (amoxicillin/clavulanic acid 500/125 mg three times daily) 24 h before dental surgery and continuing 10 days post-surgery.

The procedure for dental implant operation was the same in both the control and irradiated group. A crestal incision was made in the interforaminal region of the mandible with a mid-line buccal release incision. A full-thickness mucoperiosteal flap was raised to expose the alveolar ridge and leveled by vertical alveolotomy if required. Implant preparation was made with a 3.5 mm diameter trephine drill (2.5 mm inner diameter) (Straumann Dental Implant System; Straumann Holding AG, Switzerland) to a depth of 10 mm at both canine regions, under continuous irrigation with sterile saline. An ejector pin was used to remove the bone cylinder from the trephine drill. The obtained bone specimen per patient was selected and prepared for further analysis.

The bone specimens (sized approximately 3.5 × 10 mm) obtained from the alveolar bone of the mandible were fixed and dehydrated with increasing concentrations of ethanol and embedded in poly(methyl methacrylate) (PMMA; Merck KGaA). The fresh surface of bone revealed from the PMMA block was used for acquiring Raman spectra. For light microscopy (LM), thin sections (10 μm) were prepared and stained with Masson–Goldner trichrome. The slides were observed and photographed with a Zeiss Axiolmager M2 (Carl Zeiss Microscopy GmbH, Germany).

### Raman Spectroscopy

Raman spectra were measured from the surfaces of the PMMA bone blocks with a dispersive Raman micro-spectroscopy (Thermo DXR2xi, Thermo Fisher Scientific, U.S.A.). The wavelength of 785 nm at 20 mW laser power (source) was used for excitation. The system was equipped with 400 lines/mm grating. The spectral resolution was 5 cm<sup>-1</sup> and spectra were acquired over the 3300–50 cm<sup>-1</sup> range. The mapping of the bone specimens was performed using the 10× objective (0.25 NA). Spectra from three different areas of 30 μm × 30 μm were acquired with the following parameters: 0.01 s exposure time, 50 μm confocal pinhole aperture, 2.0 μm image pixel size, and 30 scans. Representative spectral



**Figure 1.** Representative optical micrograph of the cortical bone specimen marked with sites of spectral acquisition.

acquisition areas are shown in Fig. 1. All the spectral acquisition areas were selected under pathological supervision. A background spectrum of the embedding medium (PMMA) was also obtained under similar conditions.

### Data Analysis

Spectral preprocessing and analyses were performed using Matlab (MathWorks, v.R2017b). Spectra were interpolated to the 1800–820 cm<sup>-1</sup> range. The cosmic background was removed by filtering. The fluorescence background was removed by fitting a fourth-order polynomial function. To minimize the influence of the background, the PMMA spectrum was mathematically subtracted from the bone spectra. The mean spectrum for each group was calculated by averaging the variations at x-axis. Normalized spectra were used as input for multivariate principal component analysis (PCA). Further, to accurately identify the changes associated with irradiation, intensity of Raman bands corresponding to phosphate, carbonate, and organic contents were calculated by curve fitting using Origin 2021b software. (OriginLab, USA). Briefly, the process includes localization of sub-peaks by intensity minima in a second derivative spectrum. The sum of the squared differences between observed and computed

**Table II.** Comparison of biochemical parameters defined from Raman data between control and irradiated samples. The area of the peak values is represented as mean  $\pm$  standard deviation.

Bone biochemical parameter	Control (n = 16)	Irradiated (n = 17)	p-value
Phosphate content $\nu_1\text{PO}_4^{3-} \sim 960 \text{ cm}^{-1}$	$0.435 \pm 0.039$	$0.367 \pm 0.048$	<0.0001
Carbonate content $\nu_1\text{CO}_3^{2-} \sim 1070 \text{ cm}^{-1}$	$0.062 \pm 0.010$	$0.072 \pm 0.002$	<0.001
Mineral crystallinity 1/FWHM, $1/\sim 960 \text{ cm}^{-1}$	$0.055 \pm 0.002$	$0.061 \pm 0.002$	<0.0001
Carbonate to phosphate ratio $\sim 1070 \text{ cm}^{-1}/\sim 960 \text{ cm}^{-1}$	$0.142 \pm 0.020$	$0.197 \pm 0.039$	<0.0001
Mineral (phosphate $\sim 960 \text{ cm}^{-1}$ )/Matrix (CH <sub>2</sub> stretch $\sim 1446 \text{ cm}^{-1}$ )	$43.358 \pm 18.621$	$38.780 \pm 19.525$	>0.05 (NS)
Mineral (phosphate $\sim 960 \text{ cm}^{-1}$ )/Matrix (phenylalanine $\sim 1003 \text{ cm}^{-1}$ )	$92.249 \pm 42.861$	$41.949 \pm 24.489$	<0.0001

n: Number of samples used in each group; NS: Non-significant.

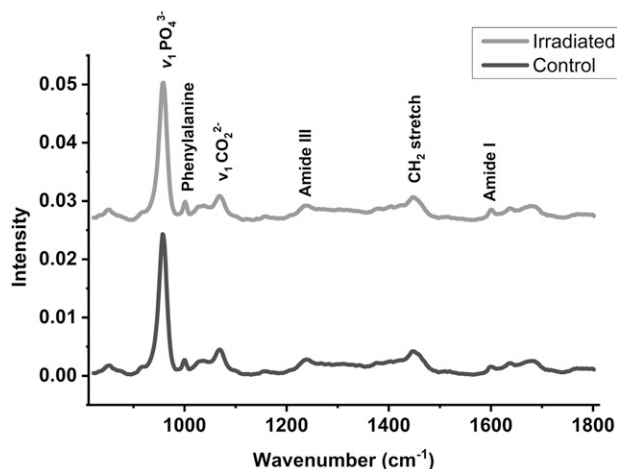


**Figure 2.** Normalized average Raman spectra from control (16) and irradiated samples (G1 + G2 = 17). Spectra are vertically offset for better visibility.

spectra was minimized to acquire the best fit.<sup>15,21</sup> An optimal Gaussian function was used for fitting and spectra band areas were calculated. Different biochemical parameters obtained from the curve-fitting analysis are shown in Table II. Mineral components were computed through the intensity of the phosphate,  $\nu_1\text{PO}_4^{3-}$  ( $\sim 960 \text{ cm}^{-1}$ ) and carbonate bands,  $\nu_1\text{CO}_3^{2-}$  ( $\sim 1070 \text{ cm}^{-1}$ ). Mineral crystallinity was obtained by computing the inverse of the full width at half-maximum (FWHM) of the phosphate band. The carbonate to phosphate ratio (CPR) was obtained to find out the carbonate substitution (B-type) rate. Matrix components were computed by using the intensity of phenylalanine ( $\sim 1003 \text{ cm}^{-1}$ ) and CH<sub>2</sub> stretch ( $\sim 1446 \text{ cm}^{-1}$ ) bands. The MMR was calculated by dividing the intensity of the phosphate band by the Phenylalanine band and the intensity of the phosphate band by the CH<sub>2</sub> stretch band. The data were expressed as the mean  $\pm$  standard deviation (SD), and comparisons were performed with unpaired Student's *t*-test coupled with Welch correction

using GraphPad Prism 6.1 software. *p*-value < 0.05 was considered as \* statistically significant; *p* < 0.01 as \*\* very significant; *p* < 0.001 and less as \*\*\* extremely significant.

## Results

A total of 16 control bone samples (46 spectra) and 17 irradiated bone samples (50 spectra) were analyzed after eliminating the spectra having detector spikes and high fluorescence background. The spectral data from both genders were pooled as no spectral differences were observed in the preliminary analysis. The average spectra from irradiated and control samples are shown in Fig. 2. Spectral variations in the spectral bands associated with mineral and matrix components were observed. These differences were further utilized for exploring the feasibility of classification using PCA. A scatter plot using scores of factors 1 and 3 is shown in Fig. 3a. As shown, two exclusive clusters belonging to control and irradiated groups were obtained. The division of the irradiated group as per the radiation dose is also visible. Loading plots of the factors used for classification shown in Fig. 3b are suggestive of differences in both mineral and matrix components of the bone. Major spectral features responsible for classification seem to be originating from phosphate and phenylalanine. The minor relative intensity associated with spectral variations among control and irradiated groups was further analyzed by curve-fitting analysis. Different spectral parameters indicating the overall bone quality and changes due to irradiation are shown in Table II.

The intensity of phosphate bands was found to be relatively less in the irradiated specimens compared to the controls. The overall intensity of the carbonate band was more in the irradiated samples. These differences were found to be statistically significant. A decrease in FWHM of the phosphate band was observed in the irradiated samples compared to controls, suggesting a significant increase in the mineral crystallinity. The irradiated samples showed a significant increase in CPR with respect to the control samples suggesting

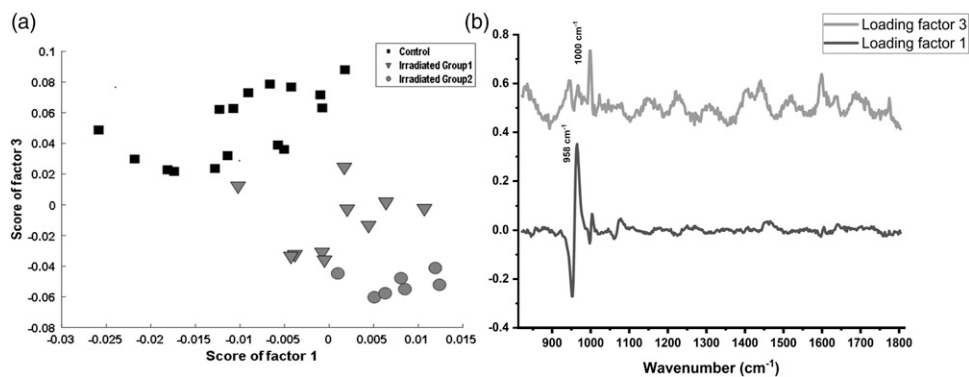


**Figure 3.** Principal component analysis between control and irradiated specimens. Group 1 (local dose < 50 Gy) and Group 2 (local dose  $\geq$  50 Gy) specimens. (a) Scatter plot and (b) loading plot of the factors used for classification.

an increase in the B-type carbonate substitution ( $p < 0.0001$ ). MMR-related parameters calculated by phosphate/phenylalanine band ratios (significant,  $p < 0.0001$ ), and the phosphate/CH<sub>2</sub> stretch band ratios (non-significant,  $p = 0.2512$ ) were reduced in the irradiated samples with respect to the controls. Further, as per the available local radiation dose data, the irradiated Group 1 ( $n = 6$ ; <50 Gy) and irradiated Group 2 ( $n = 6$ ;  $\geq$ 50 Gy) showed no differences but in comparison with the controls significant differences were observed (Fig. 4). PCA plotting based on the radiation-biopsy time interval of irradiated samples, Group A and Group B did not show any specific correlation and differences in the bone mineral and matrix contents. The details of the histological sections of the control and irradiated bone specimens as observed under LM are presented in Fig. 5.

## Discussion

The overall findings of the present study highlighted the biochemical and compositional changes due to irradiation in the human jawbone. The histological, microstructural, and vascular alterations in irradiated human mandibular bone have been previously described.<sup>22,23</sup> However, very few Raman spectroscopic studies<sup>7,15</sup> focusing on changes in the irradiated human mandibular bone are reported. Some studies have been performed on radiated animal bone tissues<sup>8,12,13,18</sup> but these data are difficult to compare with human bone as the dosage, type of radiation, and nature of bone tissue are different and the time interval of biopsy from irradiation is usually less.

A similar study by our co-author showed no significant differences between control and irradiated bone samples<sup>15</sup> despite the literature showing irradiation changes in bone. In the present study, different additional samples of the irradiated mandible were studied with a new Raman instrument having an electron multiplier charge-coupled device detector to get a higher signal with less exposure time. The spectra were collected from three areas of bone representing larger

bone specimens instead of point analysis from the previous study and therefore the present results showed significant differences.

The primary inorganic component of bone, hydroxyapatite (HA), provides strength and rigidity to the bone. Within HA, the degree of crystallinity and ion substitution governs the stiffness and the organic component, collagen, cross-link governs the toughness.<sup>1</sup> The major mineral constituents of bone observed around 960 and 1070 cm<sup>-1</sup> in Raman bands contribute to primary vibrational modes of phosphate ( $\nu_1\text{PO}_4^{3-}$ ) and carbonate ( $\nu_1\text{CO}_3^{2-}$ ). Irradiated tissue, mainly bone, presents a different degree of sensitivity. It is stated that high calcium content in bone absorbs 30–40% more irradiation than the surrounding tissues, making it a common site for radiation-induced damage.<sup>24</sup> A decrease in the intensity of phosphate band and increase in carbonate bands were observed in irradiated samples compared to controls. We suggest that RT has affected the bone minerals in our study samples.

The radiation-induced impaired mineralization and bone turnover are reflected when carbonate content (CPR) is altered.<sup>8</sup> This carbonate substitution rate has been correlated with bone maturity and aging.<sup>25</sup> Also, CPR and mineral crystallinity are spectroscopic measures of mineral crystallite size and perfection,<sup>18</sup> a result that the histopathological studies may not show. These parameters also provide information on bone growth, healing, or fragility fractures.<sup>17,26</sup> The increase in the mineral crystallinity in our irradiated group suggests mineralization with an abnormally crystalline mineral, similar to many earlier studies.<sup>8,11,13</sup> We assume that the mineral crystal size in our irradiated samples could not align well with the organic matrix and thereby making the bone weaker with respect to controls. The abnormal physiological load or unidentified underlying pathologies in the weakened irradiated mandibular bone can substantially increase the risk of fracture. Implant placement in an irradiated mandible with decreased bone mineral quality and mechanical strength can limit its success and incline to failure in the long term. The

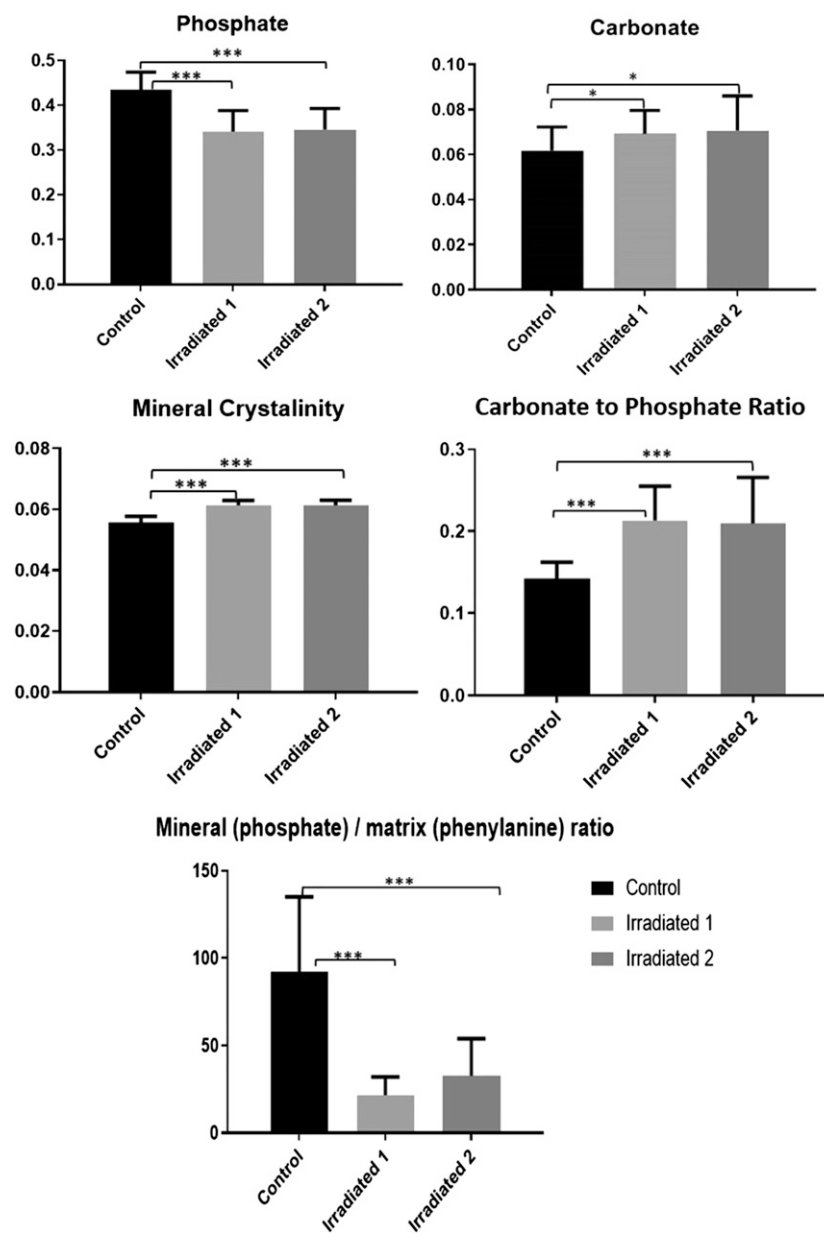


**Figure 4.** Comparison of Raman biochemical parameters between Control and Irradiated Group 1 (local dose < 50 Gy) and Group 2 (local dose  $\geq$  50 Gy) ( $p$ -value < 0.05 was considered as \* statistically significant;  $p$  < 0.01 as \*\* very significant;  $p$  < 0.001 and less as \*\*\* extremely significant).

crystallinity and carbonate substitution is increased due to the long mean radiation biopsy interval time of 63 months since it is known to increase with age.

The bone mineralization process depends on the highly regulated form of the organic matrix. It is another main compositional property related to bone mechanical strength. Both increased and decreased mineral content would degrade bone mechanical properties.<sup>27,28</sup> The amount of mineralization estimated as MMR in our irradiated samples indicates that the loss of relative mineral content in bones is higher as compared to the controls. This further causes fragility in the bone.

Phenylalanine, a short non-helical telopeptide, has been shown to catalyze the fibril formation process by aligning itself in the gap region of the type I collagen fibril and their interaction confers rigidity and stability.<sup>29</sup>  $\text{CH}_2$  band arises from organic components such as proteins, lipids, and sugars.<sup>30</sup> Phenylalanine ( $1003\text{ cm}^{-1}$ ), a band-specific to collagen, and  $\text{CH}_2$  side-chains of collagen ( $1446\text{ cm}^{-1}$ ) have shown differences with the mineral in our irradiated samples compared to control. Overall, our MMR results were decreased because radiation affected the mineral composition of bone and on the other side it also negatively affected the protein content altering the

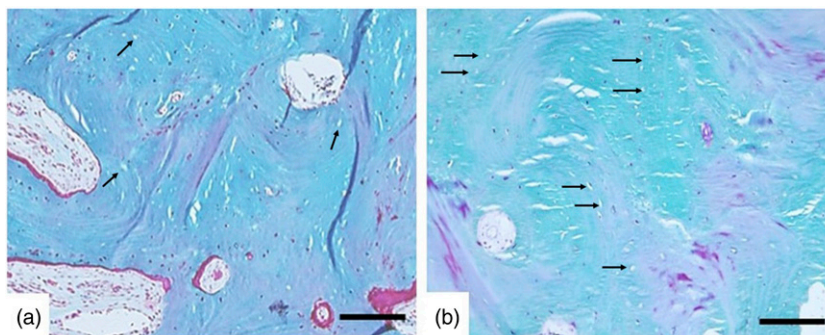


**Figure 5.** Photomicrographs showing changes in the osteocytes present in the alveolar bone of (a) the controls and (b) irradiated samples. Under light microscopy, the Masson–Goldner trichrome-stained section of controls shows Haversian canals and osteocytes within lacunae whereas the irradiated samples show fewer Haversian, and osteocytes compared to controls. Few of the osteocytic lacunae appeared empty (arrows) (Bar = 100 µm).

collagen matrix of bone. Radiation-induced structural changes in bone affecting collagen can cause disturbances in parallel packing, a reduction in their diameter breaks in collagen molecules, and abrupt intermolecular cross-links, hence resulting in premature mechanical failure of bone.<sup>20,31</sup> The structural biochemical changes are not repaired, and the bone remodeling continues with the damaged collagen scaffold. This results in bone architectural destruction and increases the incidence of the development of ORN.<sup>7,12</sup>

In some animal studies reduction in MMR in the irradiated bone was due to reduced bone formation, increased osteoclastic resorption, and compositional changes.<sup>17,32</sup> Even at the cellular level through LM the changes were evident in the irradiated samples. Osteocytes have shown a decrease in density, though they are relatively radioresistant and remain viable for several days following radiation with compromised function.<sup>33,34</sup> The long-term depletion of osteoclasts and delay in the recruitment and differentiation of new osteoblast following radiation has been shown previously.<sup>32</sup> Irradiation produces an increase in the free radicals and alters collagen synthesis, resulting in an imbalance in the bone hemostasis where the bone loses its normal cellularity and undergoes fibrosis-atrophy with impairment of its repair and remodeling capacity.<sup>35</sup> Under such conditions, even minimal dentoalveolar trauma can cause delayed healing and ulceration, facilitating contamination and infection, thus favoring bone necrosis. We believe that the compositional change observed in irradiated samples is augmented by the imbalanced interplay of the bone cells thereby complicating the post-radiation mineral/matrix assembly through the obstruction of the mineral deposition process. The decrease in cellularity of the irradiated bone could alter the bone remodeling process. The resultant damage combined with compromised vascularity might result in ORN as the long-term effect of radiation. Oral surgery after RT is a strong risk factor for the development of ORN and around 7% of ORN cases are trauma-induced.<sup>36</sup> In our study, the radiation effects were not evident clinically at the time of biopsy despite the presence of significant

biochemical changes. The hyperbaric oxygen therapy would have improved the vascularity in the irradiated mandible which raised the possibility of implant placement in our irradiated patients.

A micro-CT and histomorphometry study on irradiated mandibular bone dramatically impaired bone turnover with deterioration of trabecular microarchitecture. The 50 Gy value was a critical threshold where the radiation effects were more detrimental.<sup>23</sup> The effect of radiation-induced damage on biochemical parameters based on the dose of radiation was not significant in our irradiated subgroups. However, significant differences were observed when compared to controls. Prior administration of hyperbaric oxygen therapy for patients receiving more than 50 Gy dose could also be a factor for the non-significant subgroup differences.

We believe that ours is the third Raman spectroscopic study on the human mandibular bone to elucidate the radiation-induced damage. Our study included human irradiated bone samples with some limitations. First, the Raman mapping was done in the majority of the osteonal areas but a few interstitial areas of the cortical bone were also involved which might have resulted in a lack of differences for some Raman parameters between the study groups. Second, the radiation in the animal studies included the healthy bone, whereas in human studies the radiation was delivered as a cancer treatment modality, where the presence of cancer is another added factor in compromising bone health.

## Conclusion

Radiation exposure leads to biochemical changes in both the mineral and matrix parts of the bone, with reduced mineralization and altered collagen. The result obtained through Raman spectroscopy showed compositional changes affecting the quality and mechanical competence of the irradiated mandibular bone which might increase the risk of implant failure or fracture as a delayed complication. Further spectroscopic studies correlating with advanced histopathological

methods are required to understand the radiation-associated risks and ORN pathophysiology and to improve the clinical outcome in these irradiated patients.

### Declaration of Conflicting Interests

The author(s) declared no potential conflicts of interest with respect to the research, authorship, and/or publication of this article.

### Funding

The author(s) received no financial support for the research, authorship, and/or publication of this article.

### Data Availability Statement

All necessary data is included in this manuscript. For specific requests regarding data availability, please contact the corresponding author.

### ORCID iDs

Engelber A. J. M. Schulten  <https://orcid.org/0000-0001-8245-6367>

Surya P. Singh  <https://orcid.org/0000-0001-9984-5385>

Arja M. Kullaa  <https://orcid.org/0000-0001-8198-8185>

### References

1. S. Chauhan, S.A. Khan, A. Prasad. "Irradiation-Induced Compositional Effects on Human Bone After Extracorporeal Therapy for Bone Sarcoma". *Calif. Tissue. Int.* 2018. 103(2): 175-188.
2. D. Coletti, R.A. Ord. "Treatment Rationale for Pathological Fractures of the Mandible: A Series of 44 Fractures". *Int. J. Oral. Maxillofac. Surg.* 2008. 37(3): 215-222.
3. S. Ihde, S. Kopp, K. Gundlach, V.S. Konstantinović. "Effects of Radiation Therapy on Craniofacial and Dental Implants: A Review of the Literature". *Oral Surg. Oral Med. Oral Pathol. Oral Radiol. Endod.* 2009. 107(1): 56-65.
4. G. Granström. "Osseointegration in Irradiated Cancer Patients: An Analysis with Respect to Implant Failures". *J. Oral. Maxillofac. Surg.* 2005. 63(5): 579-585.
5. D. Oh, S.J. Huh. "Insufficiency Fracture After Radiation Therapy". *Radiat. Oncol. J.* 2014. 32(4): 213-220.
6. F. Jegoux, O. Malard, E. Goyenvalle, E. Aguado, et al. "Radiation Effects on Bone Healing and Reconstruction: Interpretation of the Literature". *Oral Surg. Oral Med. Oral Pathol. Oral Radiol. Endod.* 2010. 109(2): 173-184.
7. R.J. Lakshmi, M. Alexander, J. Kurien, K.K. Mahato, V.B. Kartha. "Osteoradionecrosis (ORN) of the Mandible: A Laser Raman Spectroscopic Study". *Appl. Spectrosc.* 2003. 57(9): 1100-1116.
8. B. Gong, M.E. Oest, K.A. Mann, T.A. Damron, et al. "Raman Spectroscopy Demonstrates Prolonged Alteration of Bone Chemical Composition Following Extremity Localized Irradiation". *Bone.* 2013. 57(1): 252-258.
9. S.R. Padala, P. Asikainen, T. Ruotsalainen, J.J. Mikkonen, et al. "Effects of Irradiation in the Mandibular Bone Loaded With Dental Implants, an Experimental Study with a Canine Model". *Ultrastruct. Pathol.* 2021. 45(4-5): 276-285.
10. C. Kendall, M. Isabelle, F. Bazant-Hegemark, J. Hutchings, et al. "Vibrational Spectroscopy: A Clinical Tool for Cancer Diagnostics". *Analyst.* 2009. 134(6): 1029-1045.
11. T. Yamamoto, K. Uchida, K. Naruse, M. Suto, et al. "Quality Assessment for Processed and Sterilized Bone Using Raman Spectroscopy". *Cell Tissue Bank.* 2012. 13(3): 409-414.
12. P.A. Felice, B. Gong, S. Ahsan, S.S. Deshpande, et al. "Raman Spectroscopy Delineates Radiation-Induced Injury and Partial Rescue by Amifostine in Bone: A Murine Mandibular Model". *J. Bone. Miner. Metab.* 2015. 33(3): 279-284.
13. C.N. Tchanque-Fossuo, B. Gong, B. Poushanchi, A. Donneys, et al. "Raman Spectroscopy Demonstrates Amifostine Induced Preservation of Bone Mineralization Patterns in the Irradiated Murine Mandible". *Bone.* 2013. 52(2): 712-717.
14. A. Palander, H. Dekker, M. Hyvarinen, L. Rieppo, et al. "Long-Term Changes in Mandibular Bone Microchemical Quality After Radiation Therapy and Underlying Systemic Malignancy: A Pilot Study". *J. Innov. Opt. Health Sci.* 2021. 14(6): 2150019.
15. S.P. Singh, I. Parviainen, H. Dekker, E.A.J.M. Schulten, et al. "Raman Microspectroscopy Demonstrates Alterations in Human Mandibular Bone After Radiotherapy". *J. Anal. Bioanal. Tech.* 2015. 6(6): 276.
16. D.E. Green, B.J. Adler, M.E. Chan, J.J. Lennon, et al. "Altered Composition of Bone as Triggered by Irradiation Facilitates the Rapid Erosion of the Matrix by Both Cellular and Physicochemical Processes". *PloS One.* 2013. 8(5): E64952.
17. J.D. Wernle, T.A. Damron, M.J. Allen, K.A. Mann. "Local Irradiation Alters Bone Morphology and Increases Bone Fragility in a Mouse Model". *J. Biomech.* 2010. 43(14): 2738-2746.
18. G.S. Mandair, M.E. Oest, K.A. Mann, M.D. Morris, et al. "Radiation-Induced Changes to Bone Composition Extend beyond Periosteal Bone". *Bone. Rep.* 2020. 28(12): 100262.
19. M.E. Oest, B. Gong, K. Esmonde-White, K.A. Mann, et al. "Parathyroid Hormone Attenuates Radiation-Induced Increases in Collagen Crosslink Ratio at Periosteal Surfaces of Mouse Tibia". *Bone.* 2016. 86: 91-97.
20. H.D. Barth, E.A. Zimmermann, E. Schaible, S.Y. Tang. "Characterization of the Effects of X-Ray Irradiation on the Hierarchical Structure and Mechanical Properties of Human Cortical Bone". *Biomaterials.* 2011. 32(34): 8892-8904.
21. S.P. Singh, C. Muralikrishna. "Raman Spectroscopic Studies of Oral Cancers: Correlation of Spectral and Biochemical Markers". *Anal. Methods.* 2014. 6: 8613-8620.
22. H. Dekker, N. Bravenboer, D. Van Dijk, E. Bloemenaa, et al. "The Irradiated Human Mandible: A Quantitative Study on Bone Vascularity". *Oral Oncol.* 2018. 87: 126-130.
23. H. Dekker, E.A.J.M. Schulten, L. Van Ruijven, H.W. Van Essen, et al. "Bone Microarchitecture and Turnover in the Irradiated Human Mandible". *J. Craniomaxillofac. Surg.* 2020. 48(8): 733-740.
24. M.M. Curi, C.L. Cardoso, H.G. De Lima, L.P. Kowalski, et al. "Histopathologic and Histomorphometric Analysis of Irradiation Injury in Bone and the Surrounding Soft Tissues of the Jaws". *J. Oral. Maxillofac. Surg.* 2016. 74(1): 190-199.

25. M.D. Morris, G.S. Mandair. "Raman Assessment of Bone Quality". *Clin. Orthop. Relat. Res.* 2011. 469(8): 2160-2169.
26. R. Ahmed, A.W.L. Law, T.W. Cheung, C. Lau. "Raman Spectroscopy of Bone Composition During Healing of Subcritical Calvarial Defects". *Biomed. Opt. Express.* 2018. 9(4): 1704-1716.
27. J.S. Yerramshetty, O. Akkus. "The Associations Between Mineral Crystallinity and the Mechanical Properties of Human Cortical Bone". *Bone.* 2008. 42(3): 476-482.
28. Y. Ling, H.F. Rios, E.R. Myers, Y. Lu, et al. "DMP1 Depletion Decreases Bone Mineralization In Vivo: An FTIR Imaging Analysis". *J. Bone. Miner. Res.* 2005. 20(12): 2169-2177.
29. K. Kar, S. Ibrar, V. Nanda, T.M. Getz, et al. "Aromatic Interactions Promote Self-Association of Collagen Triple-Helical Peptides to Higher-Order Structures". *Biochemistry.* 2009. 48(33): 7959-7968.
30. Y. Ishimaru, Y. Oshima, Y. Imai, T. Iimura, et al. "Raman Spectroscopic Analysis to Detect Reduced Bone Quality After Sciatic Neurectomy in Mice". *Molecules.* 2018. 23(12): 3081.
31. P.H.J.O. Limirio, P.B.F. Soares, E.T.P. Emi, C.C.A. Lopes, et al. "Ionizing Radiation and Bone Quality: Time-Dependent Effects". *Radiat. Oncol.* 2019. 14(1): 15.
32. M.E. Oest, V. Franken, T. Kuchera, J. Strauss, et al. "Long-Term Loss of Osteoclasts and Unopposed Cortical Mineral Apposition Following Limited Field Irradiation". *J. Orthop. Res.* 2015. 33(3): 334-342.
33. S.R. Padala, B. Kashyap, H. Dekker, J.J. Mikkonen, et al. "Irradiation Affects the Structural, Cellular and Molecular Components of Jawbones". *Int. J. Radiat. Biol.* 2022. 98(2): 136-147.
34. A. Chandra, T. Lin, J. Zhu, W. Tong, et al. "PTH1-34 Blocks Radiation-Induced Osteoblast Apoptosis by Enhancing DNA Repair through Canonical Wnt Pathway". *J. Biol. Chem.* 2015. 290(1): 157-167.
35. G.M. Hommez, G.O. De Meerleer, W.J. De Neve, R.J. De Moor. "Effect of Radiation Dose on the Prevalence of Apical Periodontitis: A Dosimetric Analysis". *Clin. Oral. Investig.* 2012. 16(6): 1543-1547.
36. S. Nabil, N. Samman. "Incidence and Prevention of Osteoradionecrosis After Dental Extraction in Irradiated Patients: A Systematic Review". *Int. J. Oral. Maxillofac. Surg.* 2011. 40(3): 229-243.